

Novel Synthetic Routes to Carbon Nitride

M. Todd, J. Kouvetakis,* and T. L. Groy

Department of Chemistry and Biochemistry, Arizona State University, Tempe, Arizona 85287

D. Chandrasekhar and David J. Smith

Center for Solid State Science, Arizona State University, Tempe, Arizona 85287

P. W. Deal

Motorola Inc., Materials Characterization Laboratory, 2200 West Broadway Road, Mesa, Arizona, 85502

Received March 1, 1995. Revised Manuscript Received April 26, 1995[®]

A novel synthetic route to amorphous C_3N_4 polymeric structures has been developed. This method involves thermal decomposition of novel molecular precursors such as $C_3N_3X_2N$ - $(SnMe_3)_2$ ($X = F, Cl$), via elimination of stable $XSnMe_3$ species, to produce thin films or bulk materials of composition C_3N_4 , the highest nitrogen content observed in C-N solids. These materials are primarily sp^2 hybridized, as indicated by vibrational, solid-state NMR, and electron-energy-loss studies, and they are likely to be excellent precursors for the high-pressure synthesis of tetrahedral C_3N_4 , the structural analog of β - Si_3N_4 . A crystal structure determination of $C_3N_3F_2N(SnMe_3)_2$ reveals that the $N(CN)_3$ framework of the molecule is planar, and all C-N bonds have virtually the same length.

Introduction

Tetrahedral C_3N_4 carbon nitride, analogous to β - Si_3N_4 , has become the focus of considerable recent research, especially because of predictions that it may have a hardness greater than that of diamond.¹ From a synthesis viewpoint, the preparation of a solid-state material that incorporates only nitrogen and carbon in the -3 and +4 oxidation states, respectively, is particularly challenging since these elements generally favor formation of multiply bonded molecular species rather than polymeric structures.² Attempts by various groups to synthesize carbon nitride have thus far yielded materials with nitrogen content considerably less than the theoretical value of 57% for C_3N_4 . These synthetic methods have included high-pressure thermal decomposition of C-H-N precursors,^{3,4} deposition using nitrogen ions and carbon vapor,⁵ plasma decomposition of methane and nitrogen,⁶ shockwave compression of organic molecules,⁷ and sputtering experiments.⁸⁻¹¹ The resulting materials have been reported to be either amorphous with very low nitrogen content or else

mixtures of extremely small crystallites dispersed in an amorphous carbon matrix. The crystallites are purported to exhibit diffraction patterns consistent with the proposed β - C_3N_4 structure.¹¹

A promising synthetic route to tetrahedral C_3N_4 involving low-temperature physical deposition techniques has been reported recently.¹² This method produced materials with 40% nitrogen incorporation by utilizing a combination of highly energetic carbon species, generated by laser ablation of pure graphite, and reactive atomic nitrogen, generated in a radio frequency discharge. It has been proposed that these nonstoichiometric materials are combinations of nanocrystallites of β - C_3N_4 and amorphous sp^2 C-N materials.¹³ Such deposits would be unsuitable for any useful characterization and would lack the unique properties of bulk C_3N_4 material. To obtain pure carbon nitride, the development of new synthetic methods to provide material with the correct bulk composition is required.

Our work has been directed toward the synthesis and use of novel molecular precursors to prepare extended carbon-nitrogen solids with the desired C:N atomic ratio of 3:4.¹⁴ Our primary aim has been to grow pure C_3N_4 polymeric materials as thin films or bulk powders, with the ultimate objective of achieving crystalline structures via high-pressure techniques. The molecular precursors have been selected to incorporate the stoichiometry of the desired product and to favor low-temperature reaction routes that are likely to lead to metastable structures and compositions. To keep the deposition temperature low, carbon and nitrogen atoms in the precursors should not contain any strong C-H

[®] Abstract published in *Advance ACS Abstracts*, June 1, 1995.

(1) Cohen, M. L. *Phys. Rev. B* **1985**, *32*, 7988.

(2) Schnick, W. *Angew. Chem., Int. Ed. Engl.* **1993**, *32*, 806-818.

(3) Maya, L.; Cole, D. R.; Hagaman, E. W. *J. Am. Ceram. Soc.* **1991**, *74*, 1686-88.

(4) Sekine, T.; Kanda, H.; Bando, Y.; Yokoyama, M.; Hojoi, K. *J. Mater. Sci. Lett.* **1990**, *16*, 1376-1378.

(5) Chubaci, J. F. D.; Sakai, T.; Yamamoto, T.; Ogata, K.; Ebe, A.; Fujimoto, F. *Nucl. Instrum. Methods Phys. Res.* **1993**, Sect. B B80-81 (Pt. 1), 463-6.

(6) Han, H.-X.; Feldman, B. J. *Solid State Commun.* **1988**, *65*, 921.

(7) Wixom, M. R. *J. Am. Ceram. Soc.* **1990**, *73*, 1973-78.

(8) Cuomo, J. J.; Leary, P. A.; Reuter, W.; Yu, D.; Frisch, M. *J. Vac. Sci. Technol.* **1979**, *16*, 299-302.

(9) Cheng, Y. M.; Lin, X.; Dravid, V. P.; Chung, Y. W.; Wong, M. S.; Sproul, W. D. *Surf. Coating Technol.* **1992**, *54/55*, 360-364.

(10) Haller, E. E.; Cohen, M.; Hansen, W. L. US Patent, 5,110,679, 1992.

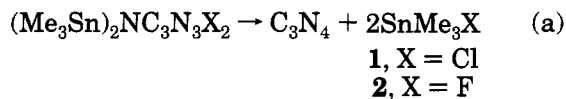
(11) Yu, K. M.; Haller, E. E.; Hansen, W. L.; Liu, A. Y.; Wu, J. C. *Phys. Rev.* **1994**, *49*, 5034-5037.

(12) Niu, C.; Lu, Y. Z.; Lieber, C. M. *Science* **1993**, *261*, 334.

(13) Marton, D.; Boyd, K. J.; Al-Bayati, A. H.; Todorov, S. S.; Rabalais, J. W. *Phys. Rev. Lett.* **1994**, *73*, 118-121.

(14) Kouvetakis, J.; Bandari, A.; Todd, M.; Wilkens, B. *Chem. Mater.* **1994**, *6*, 811-814.

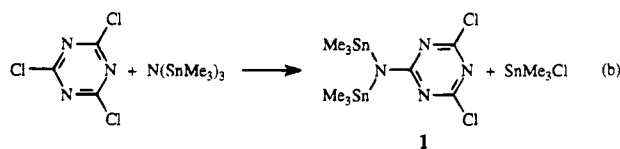
and N–H bonds. Examples of precursors possessing the correct stoichiometry and lacking strong C–H and N–H bonds (except for the trimethyl leaving groups) are $C_3N_3Cl_2N(SnMe_3)_2$ (**1**), $C_3N_3F_2N(SnMe_3)_2$ (**2**), and their trimethylsilyl analogues $C_3N_3Cl_2N(SiMe_3)_2$ (**3**), and $C_3N_3F_2N(SiMe_3)_2$ (**4**). We have previously reported the synthesis of compounds **3** and **4** and their use to deposit thin films of composition C_3N_4 – $C_{3.2}N_4$.¹⁴ In this paper we report the syntheses of precursors **1** and **2**, and then we describe their decomposition reactions via elimination of $SnMe_3Cl$ and $SnMe_3F$ (eq a), leading eventually



to deposition of thin films and bulk powders of C_3N_4 . We also compare the results obtained from the decomposition of the trimethylsilyl precursors with those of the trimethylstannyl analogues and describe the advantages of using **1** and **2** for C_3N_4 synthesis.

Results and Discussion

Precursor Synthesis. We synthesized **1** from 2,4,6-trichloro-1,3,5-triazine and tris(trimethylstannyl) amine (eq b).



Compound **1** is a colorless, highly air-sensitive solid that distills without decomposition (bp 80 °C at 10^{-2} Torr). Evidence for the six-membered cyclic structure is provided by the ¹³C spectrum which indicates the presence of two nonequivalent ring carbons (169.2 and 171.7 ppm) in the ratio 1:2 and methyl carbons of the trimethylstannyl group (–3.94 ppm). The FTIR spectrum reveals the characteristic C–H stretches of the trimethylstannyl group at 2912 and 2997 cm^{-1} , strong absorptions due to the aromatic ring at 1475–1550 cm^{-1} , and the Sn–N absorption at 790 cm^{-1} . Electron impact mass spectroscopic analysis shows $(M - CH_3)^+$ as the most intense peak at $m/e = 475$, and a fragmentation pattern that is consistent with the monosubstituted ring structure. Upon exposure to air, the material undergoes hydrolysis. Mass spectroscopic and IR analyses indicate that $Me_3SnNHC_3N_3Cl_2$ is formed first; complete hydrolysis gives rise quantitatively to $H_2NC_3N_3Cl_2$ and trimethyltin hydroxide.

In a similar manner, the reaction of 2,4,6-trifluoro-1,3,5-triazine and tris(trimethylstannyl)amine yielded compound **2** as a colorless air-sensitive solid. This compound was again characterized as the monosubstituted ring structure using FTIR, NMR, GC/MS, and elemental analyses. A single-crystal X-ray structure determination of **2** was performed using crystals obtained by sublimation (Tables 1 and 2). As shown in Figure 1, the molecule is planar with the exception of the methyl groups. The maximum deviation from the least-squares plane through the $N(CN)_3$ framework and the tin atoms is 0.09 Å. The ring is, however, slightly

Table 1. Structure Determination Summary for **2**

Crystal Data	
empirical formula	$C_9H_{18}F_2N_4Sn_2$
color; habit	colorless and irregular
crystal size (mm)	$0.20 \times 0.25 \times 0.28$
space group	$P2_1/n$
unit-cell dimensions	$a = 9.386(2)$ Å $b = 16.670(3)$ Å $c = 10.833(2)$ Å $\beta = 95.81(3)^\circ$
volume	$1686.4(8)$ Å ³
Z	4
formula weight	457.7
density (calc.)	1.803 Mg/m ³
abs coeff	2.969 mm ⁻¹
F(000)	872
Data Collection	
diffractometer used	Siemens R3m/V
radiation	Mo K α ($\lambda = 0.71073$ Å)
temp (K)	293
monochromator	highly oriented graphite crystal
2 θ range	3.5 – 45.0°
scan type	ω
scan speed	variable; 2.00 – 14.65 /min in ω
scan range (ω)	3.00°
background measurement	stationary crystal and stationary counter at beginning and end of scan, each for 25.0% of total scan time
standard reflections	3 measured every 47 reflections
index ranges	$-10 \leq h \leq 10$, $-1 \leq k \leq 17$ $0 \leq l \leq 11$
reflections collected	2565
independent reflections	2223 ($R_{int} = 3.26\%$)
observed reflections	1567 ($F > 3.0\sigma(F)$)
absorption correction	N/A
Solution and Refinement	
system used	Siemens SHELXTL PLUS (PC Version)
solution	direct methods
refinement method	full-matrix least-squares
quantity minimized	$1567 \sum w(F_o - F_c)^2$
absolute structure	N/A
extinction correction	$\chi = 0.00003(2)$, where $F^* = F[1 + 0.002 \chi F^2 / \sin(2\theta)]^{-1/4}$
hydrogen atoms	riding model, isotropic U fixed at 1.2 times the isotropic U of bonding partner
weighting scheme	$w^{-1} = \sigma^2(F) + 0.0004F^2$
no. of parameters refined	155
final R indexes (obs data)	$R = 4.88\%$, $wR = 4.56\%$
R indexes (all data)	$R = 7.91\%$, $wR = 4.98\%$
goodness-of-fit	1.24
largest and mean Δ/σ	0.008, 0.002
data-to-parameter ratio	10.1:1
largest difference peak	0.64 e Å ⁻³
largest difference hole	-0.68 e Å ⁻³

distorted.¹⁵ The N2–C3–N3 angle is 130.0° while the opposite C2–N1–C1 angle is 114.7° . This distortion from 120° presumably originates from packing effects in the solid state. The three C–N bond lengths of the ring appear to be within a normal range. The fourth C–N bond (C1–N4) has virtually the same length as the ring C–N bonds, indicating some degree of π -bonding between the ring and N4. The planar nature of the $N(CN)_3$ framework and the unusually short length of C1–N4 are consistent with a proposed two-dimensional C_3N_4 structure for which the $N(CN)_3$ unit is both the compositional and structural building block.¹⁴

Film Deposition Using **1 and **2**.** The thermal behavior of both compounds was examined by modu-

(15) Kouvetakis, J.; Grotjhan, D.; Becker, P.; Moore, S.; Dupon, R. *Chem. Mater.* **1994**, *6*, 636.

Table 2. Atomic Coordinates ($\times 10^4$) and Equivalent Isotropic Displacement Coefficients ($\text{\AA}^2 \times 10^3$) for 2

atom	x	y	z	$U(\text{eq})^a$
Sn(1)	5898(1)	2209(1)	2617(1)	60(1)
Sn(2)	2662(1)	721(1)	2487(1)	56(1)
C(1)	5706(14)	457(8)	2526(11)	56(5)
N(4)	4824(9)	1078(6)	2600(8)	53(4)
N(1)	5165(10)	-302(6)	2571(10)	66(4)
C(2)	6096(17)	-869(8)	2486(12)	68(6)
N(2)	7456(12)	-847(7)	2491(12)	76(5)
C(3)	7875(13)	-93(11)	2458(11)	65(6)
N(3)	7135(10)	571(6)	2511(9)	55(4)
F(1)	5550(8)	-1606(4)	2515(10)	118(4)
F(2)	9264(7)	17(5)	2458(8)	98(4)
C(4)	7400(16)	2191(9)	4183(11)	99(6)
C(5)	4301(14)	3054(7)	2916(16)	109(7)
C(6)	6632(14)	2299(9)	834(10)	90(6)
C(7)	2460(14)	135(9)	4172(12)	96(7)
C(8)	1357(15)	1760(9)	2389(14)	105(7)
C(9)	2243(14)	105(9)	790(11)	92(6)

^a Equivalent isotropic U defined as one-third of the trace of the orthogonalized U_{ij} tensor.

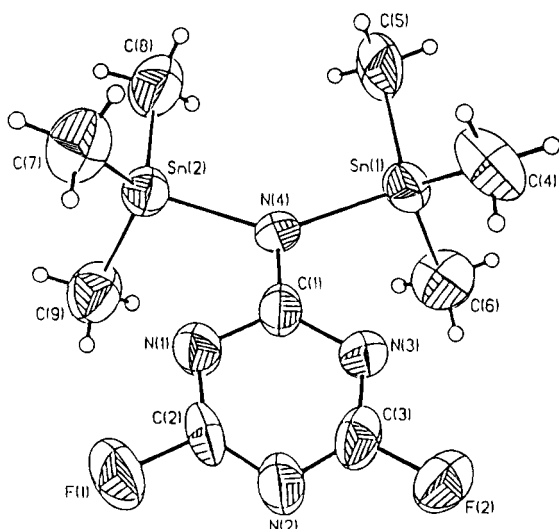


Figure 1. Molecular structure of compound **2** showing atom labeling scheme with thermal ellipsoids at 50% probability level. Important distances (\AA); angles (deg): N4-C1 1.333(16), C1-N1 1.366(16), N1-C2 1.297(18), C2-N2 1.277(20), N2-C3 1.318(20), C3-N3 1.311(19), N3-C1 1.356(16); N3-C1-N4 120.9(11), N4-C1-N1 118.8(11), C1-N1-C2 114.7(11), N1-C2-N2 131.2(12), C2-N2-C3 109.2(11), N2-C3-N3 130.0(12), C3-N3-C1 114.3(11).

lated differential scanning calorimetry (MDSC) between 0 and 500 °C. The thermograms for compounds **1** and **2** (Figure 2) revealed reversible endothermic events at 60 and 70 °C, respectively, corresponding to the melting point of the compounds, and irreversible exothermic events at 220 and 200 °C, respectively, indicative of their decomposition reactions. The decomposition reaction of compound **1** was initially carried out in a low-pressure chemical vapor deposition (CVD) reactor at 400 °C and 10^{-2} Torr to yield thin films of C_3N_4 via elimination of SnMe_3Cl . A quantitative amount of SnMe_3Cl was collected and identified by FTIR, NMR, and vapor pressure measurements. Film thicknesses of 2000–5000 \AA were deposited on Si substrates at a rate of 200–300 $\text{\AA}/\text{min}$. These films were extensively analyzed for composition and chemical purity by Rutherford backscattering (RBS) and secondary-ion mass spectrometry (SIMS). RBS analyses revealed carbon and nitrogen in a ratio of 3C to 4N with less than 1 at. % tin and chlorine impurities. Figure 3 shows the RBS

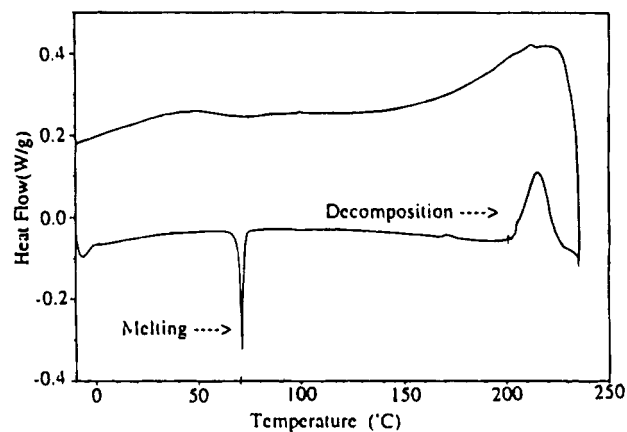


Figure 2. DSC thermogram for compound **2** shows endothermic event at 70 °C corresponding to melting point of compound, and exothermic event at 200 °C, indicative of its decomposition reaction.

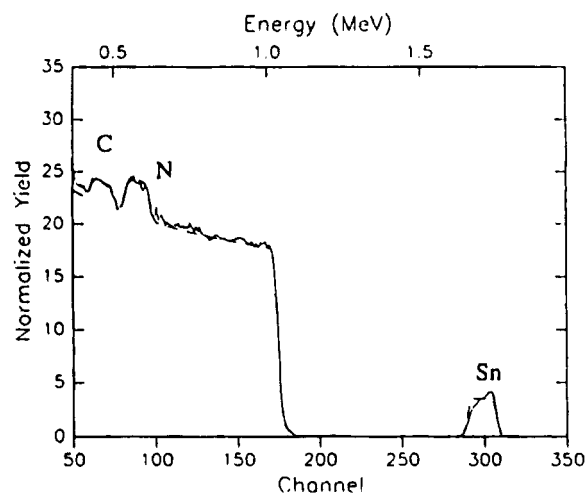


Figure 3. Rutherford backscattering spectrum of carbon nitride material deposited at 400 °C on (100) Si via decomposition of **1**. Simulation of composition using program RUMP indicates composition of $\text{C}_3\text{N}_{3.9}\text{Sn}_{0.07}$ and film thickness of 2300 \AA . Tin signal also indicates concentration gradient of element in film. Concentration appears to be higher on surface than in bulk.

spectrum of a 2300 \AA thin film on Si with composition $\text{C}_3\text{N}_{3.9}\text{Sn}_{0.07}$. (Small concentrations of Sn are easily detected by RBS because of its high atomic and mass numbers.) SIMS depth profile experiments showed that carbon and nitrogen were homogeneously distributed throughout the film and that any oxygen impurities were concentrated at the film surfaces. Infrared (IR) spectroscopic data indicated that the sp^2 1,3,5-triazine ring of the precursor persisted in the polymeric structure. IR spectra of films deposited on single crystal Si showed strong bands between 1650 and 1150 cm^{-1} which were consistent with aromatic $(\text{CN})_3$ and C-N modes. Furthermore, analysis by electron-energy-loss spectroscopy (EELS) using a 200 kV analytical electron microscope gave evidence only for carbon and nitrogen and suggested that the carbon and nitrogen were primarily sp^2 hybridized. An EELS spectrum of C_3N_4 featuring the K-shell ionization edges for both elements is shown in Figure 4. The sharp peak at the onset of each K-edge represents a π^* transition and the broad complex peak that follows is attributable to σ^* transitions. The π^* peaks are typical of sp^2 hybridization.¹⁶

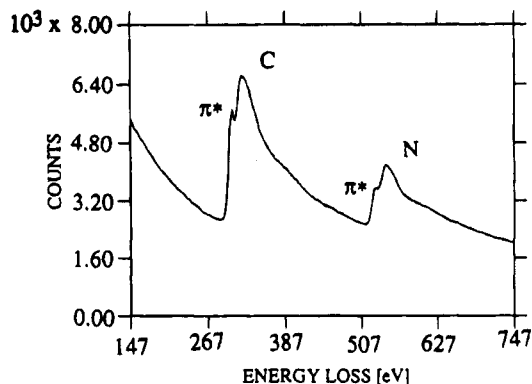


Figure 4. EELS spectrum for C_3N_4 featuring K-shell ionization edges. The π^* features indicate substantial sp^2 hybridization in both carbon and nitrogen.

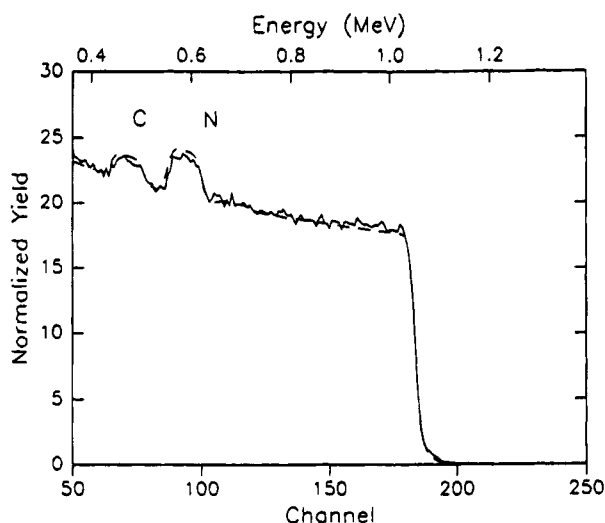


Figure 5. Typical Rutherford backscattering spectrum of carbon nitride phase deposited at 500 °C on (100) Si using **3**. Simulation of composition using program RUMP indicates carbon nitrogen ratio of 3:4.

Treatment of compound **2** in the reactor at 400–450 °C also resulted in carbon nitride thin films. The chemical composition and the bonding characteristics of this material, as indicated by RBS, SIMS, EELS, and FTIR, were similar to those of the films obtained from the decomposition of compound **1**.

Film Deposition Using **3 and **4**.** Thin films of composition C_3N_4 – $C_{3.2}N_4$ (Figure 5) having structural and bonding characteristics virtually identical to those obtained from **1** and **2** were deposited from **3** and **4** via elimination of $SiMe_3Cl$ and $SiMe_3F$ at 500 °C. The thermal behavior of compounds **3** and **4** was initially examined by DSC studies which revealed that they decomposed irreversibly at 350 and 380 °C, respectively. The deposition reactions, however, were carried out at 500 °C due to low deposition rates below 450 °C. It was also necessary to carry out the depositions of **3** and **4** at pressures ranging from 1 to 3 Torr using nitrogen as a carrier gas in order to obtain a reasonable deposition rate. In contrast, the depositions using **1** and **2** did not require a carrier gas and were carried out at much lower pressure and temperature (350–400 °C) with complete conversion of reactants to products at relatively high

deposition rates. The more facile decomposition pathway of compounds **1** and **2** (presumably due to the lower bond strength of the tin–nitrogen bond relative to the silicon–nitrogen bond) leads to low-temperature growth of high-quality nearly stoichiometric carbon nitride films. However, the $SnMe_3Cl$ and $SnMe_3F$ reaction byproducts are toxic and require special care for handling and disposing.

Sealed-Tube Decompositions. Decomposition reactions of compounds **1**–**4** were also carried out in a closed stainless-steel reactor for the purpose of obtaining bulk C_3N_4 samples for multianvil high-pressure experiments. The closed-tube decompositions of **1** and **2** at 200 °C produced volatile $SnMe_3Cl$ and $SnMe_3F$, respectively, which were collected in nearly quantitative amounts by trap-to-trap distillation and were identified by FTIR. The remaining yellow-white residues were examined by IR and RBS. The IR spectra of the solids were identical to those obtained from the thin films and the RBS analysis indicated that the carbon to nitrogen ratio was approximately 3:4. The closed-tube decompositions of **3** and **4** required higher temperatures (400–450 °C) and gave inhomogeneous mixtures of viscous oily residues and dark brown solids unlike the vapor deposition reactions that had resulted in pure carbon nitride thin films.

Conclusion

Our results indicate that compounds **3** and **4** are excellent precursors to high-quality C_3N_4 thin films; however, the trimethylstannyl precursors **1** and **2** appear to be more advantageous for bulk powder synthesis as well as being more efficient for thin film growth. Decomposition of compounds **1** and **2** appears to generate powders of carbon nitrides in bulk sealed-tube reactions at temperatures as low as 200 °C. In addition, compounds **1** and **2** deposit films at relatively low temperatures and pressures with greater deposition rates and with complete conversion of reactant to products. The drawbacks are that compounds **1** and **2** are hygroscopic and therefore difficult to handle and preserve, and their decomposition gives rise to toxic byproducts such as $SnMe_3Cl$. However, the bulk sealed-tube reactions of compounds **1** and **2** afforded enough sp^2 C_3N_4 to allow a more complete characterization of this material as well as investigation of its use as a precursor to crystalline tetrahedral C_3N_4 via high-pressure techniques and laser ablation methods. Multianvil and diamond anvil high-pressure studies are currently in progress.

Experimental Procedure

General Procedures. All reagents and precursors were handled in a nitrogen-filled glovebox (Vacuum Atmospheres Model HE493 MO20-40) or using standard Schlenk and vacuum line techniques. Infrared spectra were obtained on a Nicolet Magna 550 spectrometer from liquid samples between KBr salt plates or gas samples in a 10-cm path-length gas cell with KBr windows. 1H and ^{13}C NMR spectra were recorded at 300 and 75 MHz, respectively, on a Varian Gemini 300 NMR spectrometer. Mass spectra were obtained by GC/MS on an HP 5995 spectrometer. Elemental analyses were performed at Galbraith Laboratories (Knoxville, TN). Trimethyltin chloride and 1,3,5-trichloro-2,4,6-triazine (purchased from Aldrich Chemical Co.) and 1,3,5-trifluoro-2,4,6-triazine (purchased from Alfa Chemicals) were used without further

(16) Kouvetakis, J.; Sasaki, T.; Shen, C.; Hagiwara, R.; Lerner, M.; M. Krishnan, K.; Bartlett, N. *Synt. Met.* **1990**, *34*, 1.

purification. The deposition and film analysis procedures are essentially the same as those described in ref 14.

Synthesis of 1. A solution of tris(trimethylstannyl)amine (5.9 g, 12 mmol) in dry ether (60 mL) was added dropwise to a stirred solution of $C_3N_3Cl_3$ (2.15 g, 12 mmol) in ether (50 mL). The solution was stirred for 2 h at 0 °C, and the solvent and the resulting $SnMe_3Cl$ were removed in vacuo. The residual viscous liquid was purified by low-pressure distillation to yield **2** as a colorless solid (3.35 g, 6.8 mmol, 58%).

Mp 60 °C; bp (115 °C, 10^{-3} Torr); MS (70 eV) m/z (%) 475 (100) [$M^+ - CH_3$]; 1H NMR (300 MHz, $CDCl_3$, 25 °C, TMS) δ = 0.2466; ^{13}C NMR (75 MHz, $CDCl_3$, 25 °C) δ = -3.9432, and -6.510, -6.60, -1.3, -1.4 (weak ^{117}Sn and ^{119}Sn satellite peaks), δ = 169.215 and 171.687 (ring carbons); IR (KBr) $\nu(CH_3)$ = 2919–2967 cm^{-1} , $\nu(CN)_3$ = 1500–1618 cm^{-1} , $\nu(Sn-N)$ = 790 cm^{-1} . Elemental analysis (C, H, N, Sn) was correct.

Synthesis of 2. A solution of tris(trimethylstannyl)amine (5.5 g, 11 mmol) in dry ether (60 mL) was added dropwise to a stirred solution of $C_3N_3F_3$ (1.5 g, 11 mmol) in ether (30 mL) at 0 °C. The mixture was stirred for 2 h at 0 °C and then filtered to remove the insoluble $SnMe_3F$. Removal of the solvent in vacuo yielded a solid (3.5 g, 7.6 mmol) which was purified by short-path low-pressure distillation to afford **2** in 75% yield.

Mp 66 °C; bp (85 °C, 10^{-3} Torr); 1H NMR (300 MHz, $CDCl_3$, 25 °C, TMS) δ = 0.2231 (CH_3); ^{13}C NMR (135 MHz, C_6D_6 , 25 °C) δ = -2.930, and -1.349, -1.415, -4.439, -4.511 (weak ^{117}Sn and ^{119}Sn satellite peaks), δ = 171.018 [dd, $^1J(CF)$ = 225.28 Hz, $^3J(CF)$ = 22.9 Hz C-2, C-4] and 175.667 [t, $^3J(CF)$

= 16.0 Hz, C-6]; IR (Nujol, KBr) $\nu(CH_3)$ = 2912–2897 cm^{-1} , $\nu(C_3N_3)$ = 1475–1540 cm^{-1} , $\nu(Sn-N)$ = 790 cm^{-1} , $\nu(Sn-C)$ = 547 cm^{-1} ; MS (70 eV) m/z (%) 443 (50) [$M^+ - CH_3$]. Elemental analysis (C, H, N, Sn) was correct.

Synthesis of Tris(trimethylstannyl)amine. Tris(trimethylstannyl)amine has been previously prepared by the reaction of lithium amide and trimethyltin bromide.¹⁷ It may be also prepared in 90% yield by the reaction of potassium amide (or lithium amide) with trimethyltin chloride in anhydrous ether. Mp 22 °C; 1H NMR (300 MHz, $CDCl_3$, 25 °C, TMS) δ = 0.2075 (CH_3); IR $\nu(CH_3)$ = 2984–2916 cm^{-1} , $\nu(Sn-N)$ = 745 cm^{-1} , $\nu(Sn-C)$ = 525 cm^{-1} .

Acknowledgment. We gratefully acknowledge partial support of this work by the National Science Foundation through the NYI award to J.K. (DMR 9458047). The departmental NMR facility has been supported through NSF grants (BBS 88-04992 and CHE 88-13109).

Supporting Information Available: Lists of crystallographic data (6 pages); listing of observed and calculated structure factors (16 pages). Ordering information is given on any current masthead page.

CM950100H

(17) Sisido, K.; Kozima, S. *J. Org. Chem.* **1964**, 29, 907.